ELSEVIER

Nuclear Instruments and Methods in Physics Research B 181 (2001) 268–273

NIM B
Beam Interactions with Materials & Atoms

www.elsevier.com/locate/nimb

Characterization of microstructures formed on MeV ion-irradiated silver films on Si(1 1 1) surfaces

B. Rout [1], J. Kamila, S.K. Ghose, D.P. Mahapatra, B.N. Dev *

Institute of Physics, Sachivalaya Marg, Bhubaneswar 751 005, India

Abstract

Ag epitaxial layers on silicon single crystal surfaces, upon MeV Si ion irradiation, undergo improvement in crystalline quality. This is often associated with remarkable changes in surface morphology. Growth of micron-sized (1–30 μm) islands has been observed on epitaxial Ag(1 1 1) thin films (~100 nm), deposited on Br-passivated Si(1 1 1) surfaces, when irradiated with energetic Si ions (1–12 MeV). This shows ion beam-induced mass transport in the Ag layer. The islands on the surface of the Ag films show a variation in height, diameter and number density as a function of ion energy as well as fluence. A detailed analysis with ion microprobe and atomic force microscopy is presented. Many islands interestingly appear to have a triplet pattern – the island, a depleted region around the island and a frozen wave packet. A tentative explanation for the formation of the triplet structure is given.

PACS: 61.16.−d; 61.16.Ch; 61.80.Jh; 68.55.−a
Keywords: Electronic energy loss induced effects; Epitaxial Ag layers; Mass transport and island formation

1. Introduction

Passage of energetic ions through solids leads to the loss of energy and slowing down of the ions via elastic collisions with target nuclei and electronic excitation of the target atoms. These energy loss processes are known as nuclear energy loss (S_n) and electronic energy loss (S_e), respectively. Both S_n and S_e give rise to various modifications of the solids.

In the regime of ion energies where electronic energy loss is dominant, several interesting features of modification of solids have been observed in recent years. For amorphous materials, sample dimensions perpendicular to the ion beam appears to grow indefinitely with increasing ion fluence, whereas the sample dimension parallel to the beam shrinks [1]. Some other observed effects are wrinkles on the solid surface, surface roughening or smoothing depending on the angle of incidence [2], and directional mass transport [3]. Nonlinear near-surface lattice damage occurs in the interaction of solids with cluster ions due to

* Corresponding author. Fax: +91-674-300142.
E-mail address: bhupen@iopb.res.in (B.N. Dev).
[1] Present address: Microanalytical Research Centre, School of Physics, University of Melbourne, Parkville, Victoria 3010, Australia.

0168-583X/01/$ - see front matter
PII: S0168-583X(01)00600-0

interference in the electronic energy loss process [4].

In all previous studies of interaction of monoatomic ions with solids in the dominant S_e region, the amorphous nature of the solids has been shown to be a necessary condition for the observed effects. The crystalline metals (Al, Cu, Fe, Nb, Pt, W) and alloys did not exhibit dimensional changes upon irradiation of 360 MeV Xe ions, while all glassy metals did [1]. Formation of undulations on the irradiated surface has also been observed in amorphous materials [2,5]. Lateral mass transport has been observed in crystalline InP, however, only after the amorphization fluence is reached, showing that lateral mass transport only affects amorphous materials [6]. Crystalline noble metals such as Ag and Cu with a weak electron–phonon coupling are thought to be insensitive to S_e [7].

Here we report on several new observations in the interaction of 2–12 MeV Si ions with thin ($\sim$100 nm) oriented crystalline Ag(1 1 1) layers on Si(1 1 1) substrates. In this regime of ion energies (2–12 MeV) S_e is dominant (S_n: 0.13–0.03, S_e: 2.98–7.25 keV/nm; range: 0.9–2.6 μm in Ag). The results demonstrate the sensitivity of crystalline Ag layers to S_e. The as-grown Ag(1 1 1) layers on Br-passivated Si(1 1 1) surfaces are grainy with a mosaic distribution and a strain. RBS/channeling and X-ray diffraction experiments show the crystallinity of the Ag(1 1 1) layer [8]. The crystallinity of the Ag(1 1 1) layer additionally improves upon MeV Si ion irradiation [9]. So, our experiments involve metallic crystalline layers. In the dominant S_e regime, the problem of energy transfer from the excited electrons to the lattice ions has been considered by Wang et al. [7] within the thermal spike model, where the energy transfer from the electronic system to the lattice is driven by electron–phonon (e–p) interactions. The temperature increase in the solid is calculated by solving the coupled heat equations for the ionic and electronic subsystems. The energy transfer can raise the temperature high enough to melt and even vaporize the lattice. The e–p coupling in Ag is weak and the lattice temperature rise from the thermal spike model is not significant [7]. Yet we demonstrate the mass transport in a Ag layer leading to island formation. Mass transport in a crystalline Ag layer is probably the most unexpected from both the points of crystallinity and e–p coupling. Additionally, for the first time we report the formation of ripples in the form of wave packets near many islands.

2. Experimental

Methods of preparation of Br-passivated Si substrate have been discussed elsewhere [10–12]. About 100 nm thin Ag films were deposited (at a deposition rate of 0.2–0.3 nm/s) from a W basket onto Br–Si(1 1 1) substrates at room temperature in high vacuum (4×10^{-6} Torr). Ion irradiation and RBS measurements were performed using the 3 MV Pelletron accelerator facility in our Institute [13]. Different Ag(1 1 1)/Br–Si(1 1 1) samples, were irradiated at near-normal (7° tilt) incidence to avoid channeling with 2–12 MeV Si ions at a fluence of 5×10^{15} ions/cm^2 at room temperature. The flux was 1×10^{12} ions/cm^2/s. For uniform irradiation the ion beam has been rastered on the sample. The morphology of the irradiated Ag/Br–Si(1 1 1) samples were analyzed with optical microscopy, RBS and PIXE maps with a 2 MeV H^+ microbeam using our ion microbeam facility [14], and atomic force microscopy (AFM). The amount of Br at the Ag/Si interface is $\sim 2 \times 10^{14}$ atoms/cm^2 and its role in the present experiment may be neglected [13].

3. Results and discussion

A typical optical micrograph of irradiated samples is shown in Fig. 1. In ion irradiation, such as He or H ion implantation, usually blisters are formed on the irradiated surface. In order to reveal whether the structures seen in the optical micrograph are hollow blisters or solid islands we have used ion microprobe with RBS and PIXE measurements on several regions of the samples involving a few such structures. Typical results are shown in Figs. 2 and 3 confirming that these structures are solid Ag islands and their heights are several times the original Ag thickness in the layer. This confirms that layer-to-island mass transport

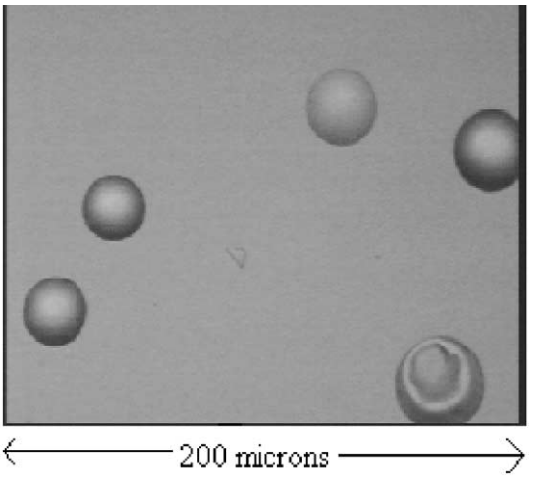

Fig. 1. Optical micrograph of islands formed in the interaction of high energy (2–12 MeV) Si ions with an epitaxial Ag layer (~100 nm) on Si(1 1 1) surfaces.

has occurred. In order to estimate the total volume (V) of the islands, we have determined the island size distribution and the average diameter (d), the number density of the islands (n) and the height-to-diameter (h/d) ratio. Representative results are shown in Fig. 4. The height-to-diameter ratio (h/d) is obtained from AFM measurements with a linear fit to data (Fig. 4(c)). A typical AFM micrograph is shown in Fig. 5. Although most of the islands are dome-shaped, some islands have a flat top like the one seen in the PIXE map of Fig. 2. Flat-top islands have also been seen in μ-RBS maps and AFM. (It should be noted that in a μ-PIXE map an actual dome-shaped island may appear to be flat-topped if the absorption length of the detected X-rays is much smaller compared to the height of the island. We have constructed the PIXE maps with Ag–L X-rays, for which the absorption length for self absorption is ~2 μm, which is larger than the island height (~1.5 μm) as seen in Fig. 3. Thus the flatness of the top in Fig. 2 is not an artifact.)

In Fig. 4(a) each point represents the average value of diameter obtained by fitting the size distribution (Gaussian) of nearly 50–150 islands. In Fig. 4(b), each point is an average of measurements on 5–10 frames of 500×500 μm^2 area, $h/d = 0.12$ (Fig. 4(c)), measured by AFM, has

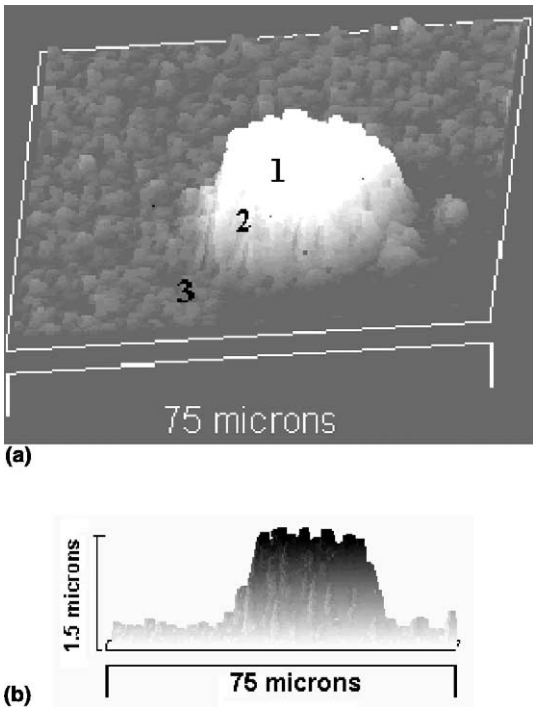

Fig. 2. (a) An elemental map (Ag-PIXE) obtained with a 2 MeV H^+ microbeam showing a Ag island. Mass depletion is seen on one side of the island. (b) A cross-sectional intensity profile obtained in a line scan across the island in (a) [in (b) black indicates the highest intensity].

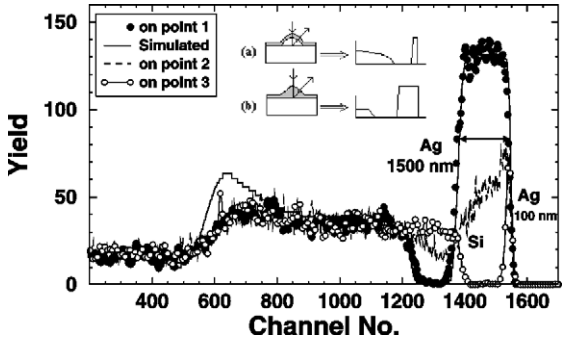

Fig. 3. RBS spectra with a 2.0 MeV proton microbeam incident at the points indicated in Fig. 2. Distinction between a hollow blister and a solid island is illustrated in the inset. The simulated spectrum includes the straggling effect.

been used to estimate the volume of the islands, assuming an island to be a section of a sphere. So the volume of the island is given by [15]

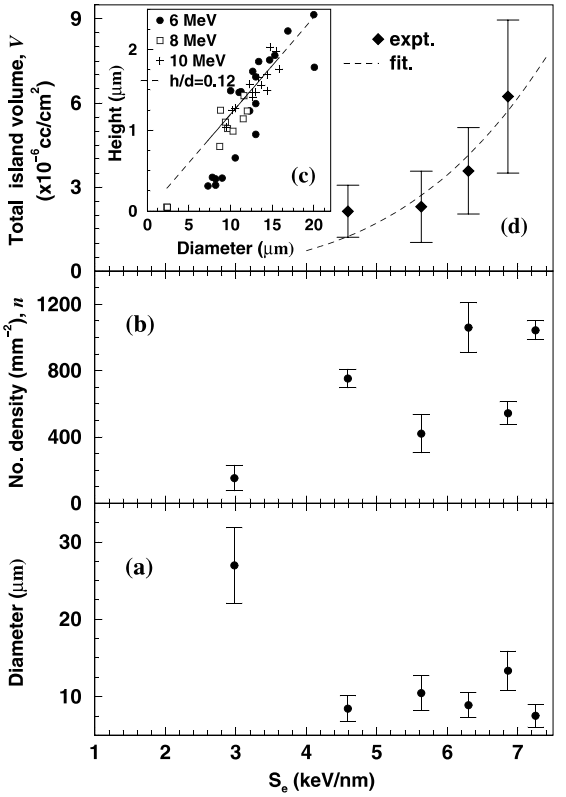

Fig. 4. (a) Average island diameter, (b) number density of islands, (c) height (h)–diameter (d) scatter plot and (d) total volume of islands as a function of S_e (for 4–10 MeV Si ions) with an empirical fit (–––).

$$\overline{V} = \frac{\pi h}{24}(4h^2 + 3d^2),$$

where d is the average diameter plotted in Fig. 4(a). Fig. 4(d) shows the total volume of the islands (in μcm^3) per cm^2 of the surface ($V = 100n \cdot \overline{V}$) versus the electronic energy loss with an empirical fit: $V = 0.0038 S_e^{3.8}$, where V is in units of $\mu cm^3/cm^2$ and S_e is in keV/nm. Limited access to AFM did not allow us to take (h/d) data for the cases $S_e = 3$ and 7.3 keV/nm, and hence the corresponding data points are not seen in Fig. 4(d).

μ-PIXE and μ-RBS studies, as shown in Figs. 2 and 3, show the islands to be solid. Assuming all the islands to be solid, V could be converted to total number (N) of Ag atoms/cm^2, using bulk Ag density. This would give $N = 0.0022 S_e^{3.8}$, where N is

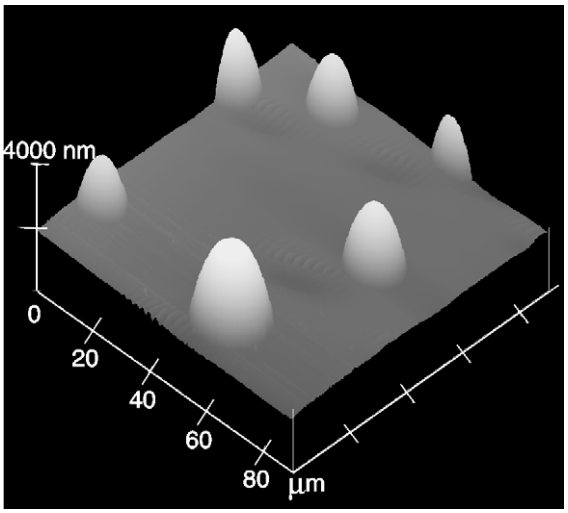

Fig. 5. A typical AFM micrograph of Ag layers on Si(1 1 1) surfaces after irradiation by 6 MeV Si ions.

in units of 10^{17} cm^{-2}. Initial Ag film thickness (~100 nm) corresponds to $\sim 5.87 \times 10^{17}$ atoms/cm^2.

μ-PIXE and μ-RBS experiments were performed on a few islands. Conventional RBS results, obtained with mm^2-sized ion beams involving a large number of islands, are not consistent with the assumption that all the islands are solid. So some islands are solid and some are hollow blisters. The solid islands are the result of mass transport from the Ag layer.

Mass transport in ion irradiation through slits has been observed by Chicoine et al. [6] in the irradiation of InP by 24 MeV heavy ions (Si, Se) at 7° incidence with respect to the surface normal. Mass depletion and accumulation have been observed at opposite edges of the slit. However, we observed mass transfer and island formation all over the uniformly irradiated sample surface. We claim that the atomic motion is set by the electronic energy deposited by ions in the system, however, the island formation has a different origin. It is the inherent strain in the epitaxial Ag layer on Si. In the heteroepitaxial growth of one material on a substrate of another material the lattice mismatch introduces a strain in the epilayer. A partial strain relaxation can occur through the formation of islands on the layer. A

classic case of such a growth process (Stranski–Krastanov growth) is Ge on Si. In the molecular beam epitaxy growth at a high substrate temperature, 3–4 uniform atomic layers are formed and further growth occurs in the form of Ge islands on this thin Ge layer. The 4% lattice mismatch between Ge and Si leads to this layer-plus-island (SK) growth instead of layer-by-layer growth [16]. Such a layer-plus-island growth appears to occur even when the growth takes place at room temperature (30°C). In this case the reduced mobility of the deposited atoms allow the formation of a relatively thick (~60 nm) strained nanocrystalline layer. Even with limited diffusion this drives the formation of nanostructural relaxed Ge islands on the Ge layer in a self-assembled process. Upon annealing at higher temperatures, the increased atomic mobility leads to an increase in the average height and the number density of Ge islands [17].

Ag grows on Si epitaxially in spite of its large lattice mismatch (25%) with Si. Apparently this is made possible by coincident site lattice matching as the lattice mismatch between $3a_{Si}$ and $4a_{Ag}$ is only 0.43% ($a_{Si} = 5.43$ Å, $a_{Ag} = 4.09$ Å) [18]. Ag deposited under high vacuum condition on Br–Si(1 1 1) substrates, just like the present case, has been found to grow epitaxially (although grainy) [8], very much like UHV deposition on clean Si(1 1 1) [18]. The quality of epitaxy improves upon thermal annealing [8] or ion beam irradiation [9]. The as-deposited layer has been found to have a strain of 0.6% [8]. We surmise, while the mobility to the Ag atoms is provided by the high electronic energy deposition, the inherent strain in the Ag layer is responsible for the Ag island formation. Strain relief via island formation [16,19] and even via island shape changes [10,11,19] are known. The edge sharpness of the Ag RBS spectrum (for point 1, Figs. 2 and 3) suggests that ion irradiation has not caused any significant intermixing and the Ag/Si interface is sharp.

Another interesting feature we have observed is the formation of frozen wave packets near the islands. These are seen in Fig. 5. Higher resolution scans are shown in Fig. 6. From cross-sectional scans over many wave packets, one of which is

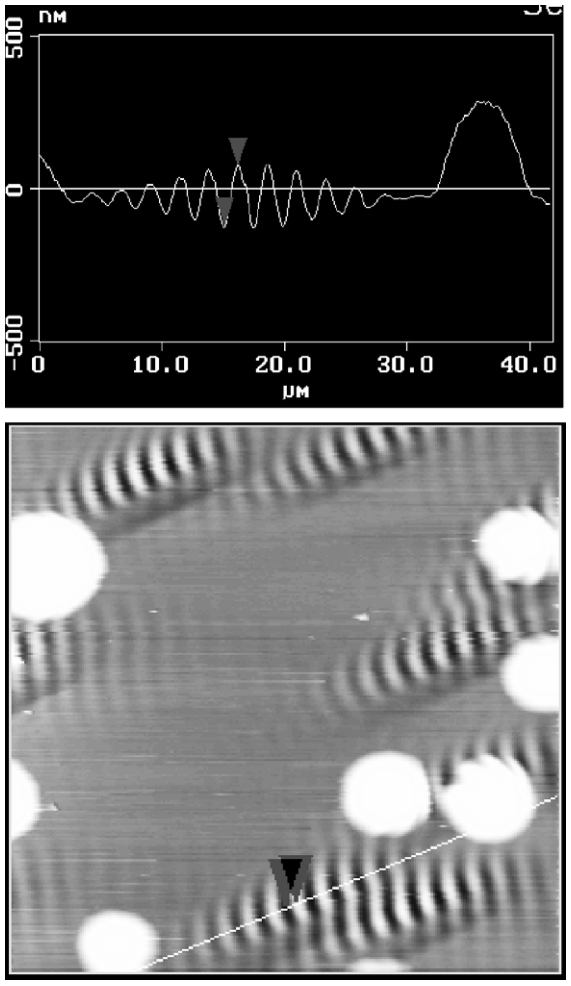

Fig. 6. A plan view (bottom) AFM micrograph showing islands and ripple formation near the islands, along with a cross-sectional view (top) of undulations along the line in the bottom micrograph.

shown in Fig. 6, the wavelength within the packet is found to be ~2.2 μm. We also notice a reduction of Ag thickness in the vicinity of the islands (see Fig. 5). A prominent case of Ag depletion around an island is also seen in Fig. 2. We conjecture that the momentum transfer from the ion to the molten solid in the trough region around the island gives rise to the formation of the displacement wave packet as seen in plan view as well as cross-sectional scan in Fig. 6. The maximum amplitude of the wave packet is about the film thickness. The

formation of wave packets may be the effect of interference between waves of slightly different wavelengths.

We believe the graininess of the crystalline Ag layer, its proximity with another material (Si) and the strain in the Ag layer are all responsible for the observed effects. Although melting is not expected in this range of S_e for crystalline Ag, presence of grain boundaries can reduce the mobility of electrons, reduce thermal conductivity and effectively raise local temperature leading to melting and mass transport.

4. Conclusions

Although in a metal like Ag with a weak e–p coupling, S_e-induced modifications are not expected even at relatively large values of S_e, we have observed S_e-induced mass transport and island formation on thin grainy epitaxial Ag layers on Si substrates over a moderate range of electronic energy loss. The mass transport apparently gives rise to a triplet structure – the island, an Ag-depleted region around the island and a frozen wave packet. We believe, the graininess, the interface with the substrate and the proximity of the thin Ag layer to a different material (substrate) are all responsible for the observed effects. More extensive studies are needed to explore the role of these parameters. In the present study ion microprobe measurements have given the vital clue about the mass transport, confirming that at least some islands seen in optical microscopy and AFM are really solid islands and not hollow blisters.

Acknowledgements

We thank Dr. B. Sundaravel for the AFM measurements on our samples. For some AFM measurements we thank also Prof. M.K. Sanyal and his group.

References

[1] M. Hou, S. Klaumunzer, G. Schumacher, Phys. Rev. B 41 (1990) 1144.
[2] A. Gutzmann, S. Klaumunzer, P. Meier, Phys. Rev. Lett. 74 (1995) 2256.
[3] L. Cliche, S. Roorda, M. Chicoine, R.A. Masut, Phys. Rev. Lett. 75 (1995) 2348.
[4] S.K. Ghose, G. Kuri, A.K. Das, B. Rout, D.P. Mahapatra, B.N. Dev, Nucl. Instr. and Meth. B 156 (1999) 125.
[5] H. Trinkaus, A.I. Ryazanov, Phys. Rev. Lett. 74 (1995) 5072.
[6] M. Chicoine, S. Roorda, L. Cliche, R.A. Masut, Phys. Rev. B 56 (1997) 1551.
[7] Z.W. Wang, Ch. Dufour, E. Paumier, M. Toulemonde, J. Phys.: Condens. Matter 6 (1994) 6733.
[8] B. Sundaravel, A.K. Das, S.K. Ghose, K. Sekar, B.N. Dev, Appl. Surf. Sci. 137 (1999) 11.
[9] B. Sundaravel, A.K. Das, S.K. Ghose, B. Rout, B.N. Dev, Nucl. Instr. and Meth. B 156 (1999) 130.
[10] K. Sekar, G. Kuri, P.V. Satyam, B. Sundaravel, D.P. Mahapatra, B.N. Dev, Surf. Sci. 339 (1995) 96.
[11] K. Sekar, G. Kuri, P.V. Satyam, B. Sundaravel, D.P. Mahapatra, B.N. Dev, Phys. Rev. B 51 (1995) 14,330.
[12] K. Sekar, G. Kuri, D.P. Mahapatra, B.N. Dev, J.V. Ramana, S. Kumar, V.S. Raju, Surf. Sci. 302 (1994) 25.
[13] K. Sekar, P.V. Satyam, G. Kuri, D.P. Mahapatra, B.N. Dev, Nucl. Instr. and Meth. B 73 (1993) 63.
[14] B. Rout, S.K. Ghose, D.P. Mahapatra, B.N. Dev, H. Bakhru, A.W. Haberl, Nucl. Instr. and Meth. B 181 (2001) 110.
[15] M. Vygodsky, in: Mathematical Handbook, MIR Publishers, Moscow, 1972, p. 326.
[16] D.J. Eaglesham, M. Cerullo, Phys. Rev. Lett. 64 (1990) 1943.
[17] A.K. Das, S.K. Ghose, B.N. Dev, G. Kuri, T.R. Yang, Appl. Surf. Sci. 165 (2000) 260.
[18] F.K. LeGouse, M. Liehr, M. Renier, W. Krakow, Philos. Mag. B 57 (1988) 179.
[19] J. Tersoff, R.M. Tromp, Phys. Rev. Lett. 70 (1993) 2782.